Spinons in the Strongly Correlated Copper Oxide Chains in $SrCuO_2$

I. A. Zaliznyak,[1] H. Woo,[1,2] T. G. Perring,[2] C. L. Broholm,[3] C. D. Frost,[2] and H. Takagi[4]
[1]*Brookhaven National Laboratory, Upton, New York 11973-5000, USA*
[2]*ISIS Facility, Rutherford Appleton Laboratory, Chilton, Didcot OX11 0QX, United Kingdom*
[3]*Department of Physics and Astronomy, The Johns Hopkins University, Baltimore, Maryland 21218, USA*
[4]*Graduate School of Frontier Sciences and Institute for Solid State Physics, University of Tokyo, and CREST-JST, Hongo, Tokyo 113-8656, Japan*
(Received 31 December 2003; published 16 August 2004)

We have investigated the spin dynamics in the strongly correlated chain copper oxide $SrCuO_2$ for energies up to $\gtrsim 0.6$ eV using inelastic neutron scattering. We observe a gapless continuum of magnetic excitations, which is well described by the "Müller ansatz" for the two-spinon continuum in the $S = 1/2$ antiferromagnetic Heisenberg spin chain. The lower boundary of the continuum extends up to $\approx$ 360 meV, which corresponds to an exchange constant $J = 226(12)$ meV.

DOI: 10.1103/PhysRevLett.93.087202 PACS numbers: 75.40.Gb, 71.27.+a, 75.10.Jm, 75.10.Pq

The unique properties of the one-dimensional (1D) electronic systems in copper based chain materials continue to attract theoretical and experimental attention. Not only are they a test bed for understanding the unusual electronic properties of high-T_c superconductors, they also allow experimental access to fundamental physical phenomena in one dimension, such as the 1D Mott insulator, spin-charge separation, non-Fermi-liquid (Luttinger liquid) behavior, and Peierls instabilities [1–4].

The corner-sharing chain cuprate $SrCuO_2$ and its sister material Sr_2CuO_3 are of particular interest. They feature coplanar CuO_4 square plaquettes arranged so Cu^{2+} chains extend diagonally through $\approx 180°$ Cu-O-Cu bonds. Although the hopping integral t for the Cu^{2+} $3d$ electron in this geometry is large, in 1D the on-cite Coulomb repulsion U always stabilizes a Mott insulating (MI) state [1,2]. A similar bond arrangement occurs in the high-T_c cuprates, where the corner-sharing chains form a 2D square lattice of corner-sharing plaquettes. An intermediate situation that may approximate the magnetic effects of stripes in high-T_c materials [5] is found in the homologous series $Sr_nCu_{n+1}O_{2n+1}$ [6], where spin chains form $(n + 1)$-leg ladders. A "one-leg ladder," i.e., a single chain, is the simplest representation of the whole universality class of odd-rung spin ladders [7].

Supersonic spin excitations are central to understanding the low-energy electronic properties of cuprates [8–10]. Spin waves in the high-T_c parent material La_2CuO_4 have recently been characterized comprehensively by magnetic inelastic neutron scattering (INS) [11]. A two-dimensional (2D) dispersion relation corresponding to a nearest-neighbor Heisenberg spin coupling $J \approx 140$ meV *and* a four-spin cyclic exchange $J_c \approx 38$ meV was observed. The substantial cyclic exchange is a spectacular consequence of the electron itineracy in the underlying 2D Hubbard Hamiltonian. The significantly larger exchange interactions in the chain copper oxides as compared to their planar high-T_c relatives is one of the mysteries in the electronic structure of cuprates [10,12]. An accurate, direct measurement of J is vital for solving this problem, as values determined by different indirect techniques differ appreciably. The temperature dependence of the magnetic susceptibility up to 800 K suggests $J = 181(17)$ meV and $J = 190(17)$ meV in $SrCuO_2$ and Sr_2CuO_3, respectively [13], while midinfrared absorption data yield an $\approx 37\%$ larger value $J \approx 260$ meV [14]. Such a large exchange constant implies that the spinon-velocity is not much smaller than the Fermi velocity. The question therefore naturally arises whether or not spin excitations couple to charge excitations in these materials. Is it at all appropriate to describe a spin excitation in terms of a simple Heisenberg spin Hamiltonian when there is no energy-scale separation between the spin and charge sectors [3]? Here we report a neutron scattering study of spin excitations in the chain copper oxide $SrCuO_2$ which addresses these issues and provides an accurate value for J, as sought by theorists for some time [7,10,12].

$SrCuO_2$ has a centered orthorhombic crystal structure (space group $Cmcm$) with lattice parameters $a = 3.556(2)$ Å, $b = 16.27(4)$ Å, $c = 3.904(2)$ Å. The corner-sharing Cu-O chains run along the $\boldsymbol{c}$ axis and come in pairs, stacked along the $\boldsymbol{b}$ direction [15]. The coupling between chains in a pair proceeds through $\approx 90°$ Cu-O-Cu bonds and is extremely weak and frustrated [6,7]. Therefore, $SrCuO_2$ is essentially a single-chain compound, similar to Sr_2CuO_3. In both materials the interchain couplings are very small. In $SrCuO_2$ short-range static spin correlations develop below $T_N \approx 5$ K, and weak modulation of spin fluctuations in the direction perpendicular to the chains occurs only for energies $E \lesssim 2.5$ meV [15].

Measuring spin excitations at energies as high as $\sim$0.5 eV by INS only recently became a realistic possibility with the development of the MAPS spectrometer at ISIS. A $SrCuO_2$ sample with mosaic $\eta \approx 0.5°$ and $m \approx 3.9$ g, previously studied in Ref. [15], was mounted in a He-filled Al can, and cooled to $T = 12(2)$ K in a

closed cycle refrigerator. The sample was aligned with its $(h0l)$ reciprocal lattice plane horizontal and with the $\boldsymbol{c}$ axis (chain direction) perpendicular to the incident neutron wave vector $\mathbf{k}_i$. It was fully illuminated by the $\approx 45 \times 45$ mm^2 incident neutron beam. We index wave vector transfer $\boldsymbol{Q}$ in the *Cmcm* orthorhombic reciprocal lattice as (Q_h, Q_k, Q_l) and define the equivalent in-chain wave vector for the unit lattice spacing through $q = 2\pi Q_l$. The magnetic cross section was normalized using incoherent nuclear scattering from a vanadium standard.

Data were collected for incident neutron energies $E_i = 98$, 240, 517, and 1003 meV and with the frequency of the Fermi chopper chosen to have fairly coarse energy resolution (FWHM $\sim$ 5%–10% of E_i over the energy windows in Fig. 1) in order to maximize neutron flux. This is important because the magnetic intensity is very weak for high energy transfers, where a large Q is required to satisfy the energy and the momentum conservation, and an exponentially small Cu^{2+} form factor suppresses the magnetic scattering cross section. The data for different E_i shown in Figs. 1(a)–1(d) focus on different ranges of energy transfer. The onset of the magnetic scattering at a highly dispersive *lower* boundary, $\sim J \sin(q)$, is clearly observed in Figs. 1(b)–1(d). For $E_i = 98$ meV, Fig. 1(d), the steep dispersion is completely unresolved due to the coarse Q resolution imposed by the sample mosaic, $\Delta Q \approx \eta k_i$. As a result, the scattering looks like a rod, centered for all energies at $Q_l = 2n + 1$, where n is an integer [i.e., $q = \pi(2n + 1)$]. The splitting of the rod into two branches becomes visible at $E \sim 200$ meV in Fig. 1(c), and is apparent in Fig. 1(b), which shows the top of the dispersion of the *lower* boundary at $E \sim 360$ meV. On the other hand, the data for $E_i = 1003$ meV in Fig. 1(a) clearly show that the scattering continuum persists up to an *upper* boundary, which is consistent with the dispersion $\sim J \sin(q/2)$.

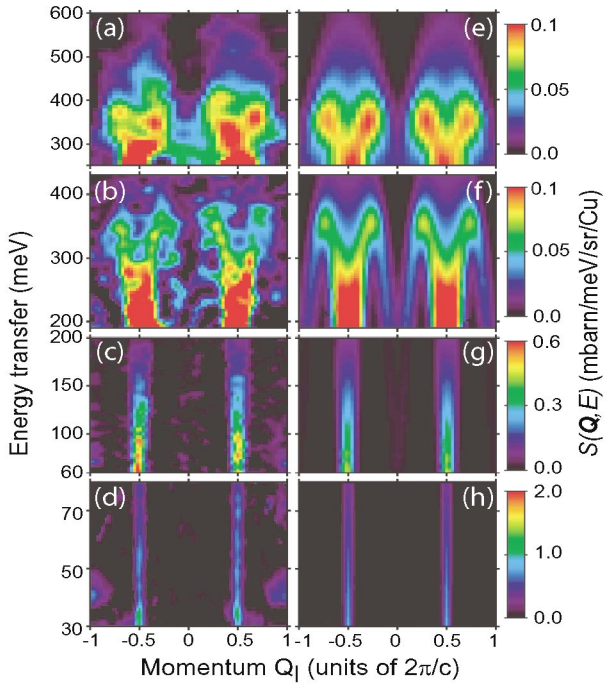

FIG. 1 (color). Color contour maps of the normalized scattering intensity projected on the (Q_l, E) plane, measured in $SrCuO_2$ for (a) $E_i = 1003$ meV, $|Q_k| < 7$; (b) $E_i = 517$ meV, $|Q_k| < 5$; (c) $E_i = 240$ meV, $|Q_k| < 5$; (d) $E_i = 98$ meV, $|Q_k| < 4$. An energy-dependent, but Q-independent, nonmagnetic background scattering, measured at $Q_l \approx 0$, was subtracted. The corresponding resolution-corrected intensity calculated from the Müller ansatz (4) is shown on the right (e)–(h).

The simplest framework for understanding the essential electronic properties of the cuprate materials is provided by an effective single-band Hubbard model [8–10,16–18]. In the 1D case, relevant for the chain cuprates, the Hamiltonian reads

$$\mathcal{H}_e = -t\sum_{j,\sigma}(c^\dagger_{j,\sigma}c_{j+1,\sigma} + \text{H.c.}) + U\sum_j n_{j,\uparrow}n_{j,\downarrow}. \quad (1)$$

Here $\sigma = \uparrow, \downarrow$, $c^\dagger_{j,\sigma}$, $c_{j,\sigma}$ are the electron creation/annihilation operators at site j along the chain, and t and U are the nearest-neighbor hopping integral and the on-site Coulomb interaction, respectively. In the undoped stoichiometric materials there is one electron per site; i.e., the band is half filled.

For very large U the electron hopping is suppressed and the lattice sites are effectively uncoupled. The system for any spatial dimension is a narrow-band, wide-gap Mott-Hubbard insulator. In this limit, $2t/U \ll 1$, an energy-scale separation occurs, where a charge gap $\sim U$ separates a $\sim 2t$ wide conduction band from the low-energy, spin part of the electronic spectrum with much smaller bandwidth $\sim 2t(2t/U)$. The latter is described by an *effective Heisenberg spin-1/2 Hamiltonian,*

$$\mathcal{H} = J\sum_j \mathbf{s}_j\mathbf{s}_{j+1}, \quad (2)$$

with exchange coupling $J = 4t^2/U[1 + O(2t/U)]$ [10]. Such a situation occurs in many strongly correlated charge-transfer insulators, e.g., in $KCuF_3$ [19]. In spite of the fundamentally different physical origin, it essentially resembles a band insulator: the electrons are strongly confined, and the low-energy spin waves are effectively decoupled from the high-energy charge excitations.

In the corner-sharing copper oxides U/t is not as large as, for example, in $KCuF_3$, and the correlation energy is comparable to the hopping kinetic energy. Such proximity to the Mott metal-insulator transition is believed to be crucial for the appearance of high temperature superconductivity upon doping [8,9]. A significant electron itineracy in 2D has immediate consequences for the spin-wave spectrum. This was recently observed in La_2CuO_4 [11], where $U \approx 2.2$ eV, $t \approx 0.30$ eV, and the band of spin excitations extends to ≈ 0.30 eV (i.e., the nearest neighbor exchange coupling is $J \approx 140$ meV), which is non-negligible compared to the charge gap. As

a result, a simple bilinear Heisenberg spin Hamiltonian such as Eq. (2) is inadequate, requiring nonphysical values of the superexchange constants. An excellent account of the data was, however, obtained by including four-spin cyclic exchange, $J_c \sim 0.3J$, which appears in fourth-order perturbation theory for the 2D Hubbard Hamiltonian.

The energy-scale separation between the spin and the charge sectors of the electronic excitation spectrum is essentially absent in chain cuprates with $\approx 180°$ Cu-O-Cu bonds. Already, it is clear from the data of Fig. 1 that the top of the lower bound of the spin excitation continuum is at $\sim$360 meV, resulting in J of $\sim$220 meV in the spin Hamiltonian (2). The triplet spin excitations bandwidth of $\pi J \approx 0.72$ eV equals about half of the optic gap, $\Delta_c \approx 1.42$ eV, corresponding to particle-hole charge excitations [20,21]. If the spin sector of the 1D Hubbard Hamiltonian (1) in such a situation can still be adequately described by the simple $S = 1/2$ Heisenberg spin Hamiltonian (2), the spin excitation spectrum must be almost entirely composed of pairs of the free, spin-1/2, "fractional" elementary excitations called spinons. They form a continuum bounded by the des Cloiseaux–Pearson (dCP) dispersion relations [22],

$$\frac{\pi}{2} J|\sin(q)| \le \varepsilon(q) \le \pi J|\sin(q/2)|. \quad (3)$$

Although the exact ground state of (2) was determined a long time ago [23], an exact expression for the two-spinon contribution to the dynamic spin structure factor $S(q, \varepsilon)$ was obtained only recently [24]. The expression differs only very slightly from the approximate, semi-empirical "Müller ansatz" (MA) expression [25],

$$S_{\mathrm{MA}}(q, \varepsilon) = \frac{A}{2\pi} \frac{\theta(\varepsilon - \varepsilon_L(q))\theta(\varepsilon_U(q) - \varepsilon)}{\sqrt{\varepsilon^2 - \varepsilon_L(q)^2}}, \quad (4)$$

which is based on consistency with sum rules and numerical simulations. Here, $\theta(x)$ is a step function, $\varepsilon_{L,U}(q)$ are the lower and the upper dCP boundaries of Eq. (3), and $A \sim 1$ is a prefactor introduced in Ref. [25], which we refine in a fit. MA (4) is routinely used to describe the two-spinon scattering, e.g., in $KCuF_3$ [19]. Although it disagrees with the exact result [24] by predicting a step-like singularity at the upper dCP boundary [26], this artifact often disappears upon convolution with the instrument resolution function. We compare our data with the $S_{\mathrm{MA}}(q, \varepsilon)$, weighted by $(\gamma r_0)^2 N \frac{k_f}{k_i} |\frac{g}{2} F(\mathbf{Q})|^2$ as appropriate for the scattering cross section, and corrected for MAPS resolution [27]. Here $(\gamma r_0)^2 = 0.290$ barn, N is the number of Cu^{2+} ions, k_i and k_f are the incident and the scattered neutron wave vectors, $g \approx 2$ is the Landé g factor, and $F(\mathbf{Q})$ is the magnetic form factor.

Each data set in Figs. 1(a)–1(d) was divided into a series of constant-E cuts, which were independently fitted to the MA cross section described above to obtain a pair of values A, J for each cut. A representative set of cuts with the corresponding fits is shown in Figs. 2 and 3. We obtain reasonably good fits, with A and J scattered within $\lesssim 20\%$ of their average values $J = 226(12)$ meV and $A = 0.55(6)$. The values and the error bars obtained from the fits are plotted in Fig. 4. The average values and the errors for A and J were obtained by performing the weighted average of the data shown in the figure (for J the $E_i = 98$ meV data were not included, as the dispersion of the spinon dCP boundary is unresolved).

We found it very important to use the anisotropic magnetic form factor appropriate for the Cu^{2+} spins in the $3d_{x^2-y^2}$ orbitals [28]. If the spherical form factor corresponding only to the j_0 term [28] is used, then the values of A for constant-energy cuts centered on similar energies, but taken from data sets with different E_i, differ by up to a factor of $\gtrsim 5$. This is because the same triplet energy is measured at different $\mathbf{Q}$, making the data sensitive to the real space distribution of the spin density.

Our findings show that up to at least 0.6 eV spin dynamics in $SrCuO_2$ is, indeed, well described by the MA for the two-spinon triplet continuum appropriate for a spin Hamiltonian (2). This is also apparent from the remarkable similarity of the contour maps of the mea-

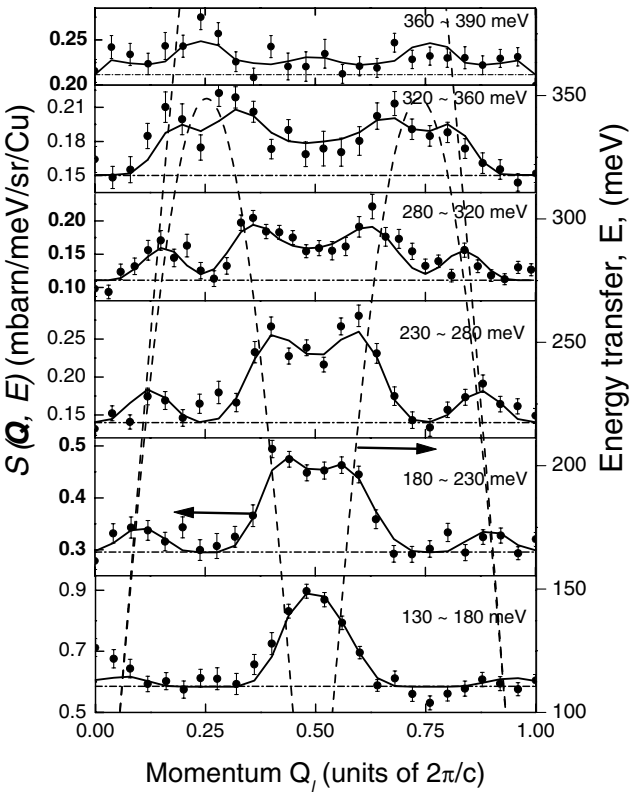

FIG. 2. Constant-E cuts of the measured scattering intensity of Fig. 1, which show the lower boundary of the spinon continuum. The intensity in each panel is combined within the energy range shown in the upper right corner. Solid lines are the fits to the resolution-corrected MA cross section (4). The broken lines are the calculated dCP boundaries (3). Dash-dotted lines show the Q-independent nonmagnetic scattering.

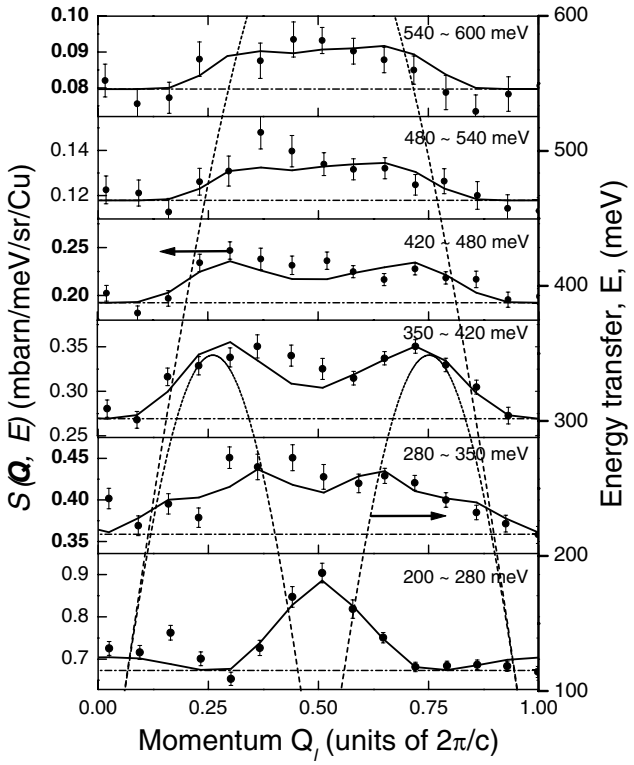

FIG. 3. Cuts of the measured scattering intensity of Fig. 1(a), which probe the upper boundary of the spinon continuum. Curves and annotations are the same as in Fig. 2.

sured intensity in Figs. 1(a)–1(d), to the corresponding resolution-corrected intensity calculated from the MA cross section and shown in the right panel of Figs. 1(e)–1(h). The experimental value for A is noticeably smaller than the value $A = 1.347$ for which Eq. (4) accounts for

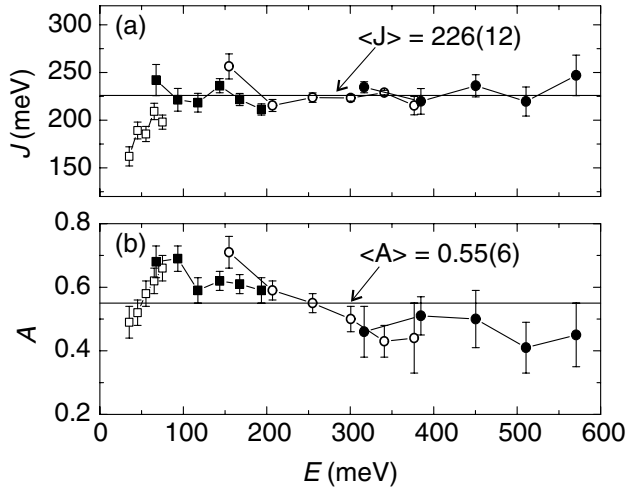

FIG. 4. Parameters (a) J and (b) A refined by fitting cuts at different E, including those in Figs. 2 and 3. The symbols □, ■, ○, and ● correspond to cuts taken with neutron energies 98, 240, 517, and 1003 meV, respectively.

the total spectral weight of a spin-1/2 degree of freedom per site [25]. At present it is unclear whether this discrepancy results from limitations in high-Q form factor extrapolations or is a subtle effect of charge fluctuations.

In summary, we have provided a detailed map of spin excitations in the chain cuprate $SrCuO_2$ for energies up to $\gtrsim 0.6$ eV. Apart from possibly an overall scale factor, the inelastic magnetic neutron scattering data are indistinguishable from those projected for a spin-1/2 Heisenberg Hamiltonian (2) with $J = 226(12)$ meV. Because spin and charge energy scales are similar in $SrCuO_2$, these data provide experimental support for spin-charge separation in one-dimensional Mott Hubbard insulators.

We thank F. Essler, A. Tsvelik, J. Tranquada, R. Coldea, D. T. Adroja, and A. Zheludev for discussions. This work was supported under DOE Contract No. DE-AC02-98CH10886. The work at JHU was supported by NSF DMR-0306940.

[1] E. H. Lieb and F. Y. Wu, Phys. Rev. Lett. **20**, 1445 (1968).
[2] F. H. L. Essler and A. M. Tsvelik, Phys. Rev. B **65**, 115117 (2002).
[3] A. Luther and V. J. Emery, Phys. Rev. Lett. **33**, 589 (1974).
[4] F. D. M. Haldane, Phys. Rev. Lett. **45**, 1358 (1980); J. Phys. C **14**, 2585 (1981).
[5] J. M. Tranquada *et al.*, Nature (London) **375**, 561 (1995).
[6] K. Ishida *et al.*, Phys. Rev. B **53**, 2827 (1996).
[7] T. M. Rice, Physica B (Amsterdam) **241–243**, 5 (1998).
[8] P. W. Anderson, Science **235**, 1196 (1987); Phys. Rev. Lett. **64**, 1839 (1990).
[9] J. Orenstein and A. J. Millis, Science **288**, 468 (2000).
[10] S. Maekawa and T. Tohyama, Rep. Prog. Phys. **64**, 383 (2001).
[11] R. Coldea *et al.*, Phys. Rev. Lett. **86**, 5377 (2001).
[12] Y. Mizuno, T. Tohyama, and S. Maekawa, Phys. Rev. B **58**, R14 713 (1998).
[13] N. Motoyama *et al.*, Phys. Rev. Lett. **76**, 3212 (1996).
[14] H. Suzuura *et al.*, Phys. Rev. Lett. **76**, 2579 (1996).
[15] I. A. Zaliznyak *et al.* Phys. Rev. Lett. **83**, 5370 (1999).
[16] A strong Cu($3d_{x^2-y^2}$)-O($2p_\sigma$) hybridization may imply a nontrivial mapping of the highest occupied Zhang-Rice singlet onto the lower Hubbard band; see Refs. [10,17,18].
[17] K. Penc and W. Stephan, Phys. Rev. B **62**, 12 707 (2000).
[18] Y. Mizuno *et al.*, Phys. Rev. B **62**, R4769 (2000).
[19] D. A. Tennant *et al.*, Phys. Rev. Lett. **70**, 4003 (1993).
[20] H. Fujisawa *et al.*, Phys. Rev. B **59**, 7358 (1999).
[21] T. Ogasawara *et al.*, Phys. Rev. Lett. **85**, 2204 (2000).
[22] J. des Cloizeaux and J. J. Pearson, Phys. Rev. **128**, 2131 (1962).
[23] H. A. Bethe, Z. Phys. **71**, 265 (1931).
[24] A. H. Bougourzi *et al.*, Phys. Rev. B **54**, R12 669 (1996).
[25] G. Müller *et al.*, Phys. Rev. B **24**, 1429 (1981).
[26] M. Karbach *et al.*, Phys. Rev. B **55**, 12 510 (1997).
[27] T. G. Perring, TOBYFIT version 2.0 (unpublished).
[28] S. Shamoto *et al.*, Phys. Rev. B **48**, 13 817 (1993).